WARSAW UNIVERSITY OF TECHNOLOGY Index 351733
FACULTY OF CIVIL ENGINEERING
COMMITTEE FOR CIVIL AND WATER ENGINEERING
POLISH ACADEMY OF SCIENCES ISSN 1230-2945

DOI: 10.24425/ace.2026.157468
ARCHIVES OF CIVIL ENGINEERING
Vol. LXXII ISSUE 1 2026

pp. 185 –206

Research paper

Investigation on the force and deformation of tunnel lining structure under the different local high water pressures

Chaojie Miao[1], Zonglong Zhang[2], Zhuoxin Liu[3], Xuebin Hu[4], Yehao Wang[5], Liang Cheng[6], Wenfeng Zhang[7]

Abstract: The water-filled caves are extremely detrimental to the stability of tunnel lining structure under the action of local high water pressures. In this paper, numerous tunnel models subjected to water pressures with different action conditions were established based on FLAC3D software. The influences of the magnitude, range, and action location of local water pressures on the internal force and deformation properties, and stability of tunnel lining structure were obtained by analyzing the bending moment and axial force, horizontal and vertical displacements, and safety factor. The results show that the bending moment and axial force, and displacement of tunnel lining structure are overall symmetrically distributed when water pressures act on tunnel vault. The maximum internal force and displacement basically occur on tunnel vault and increase significantly with the increase of water pressure and its action range; while the internal force and displacement values in other locations increase slightly with different amplitudes. The tunnel vault is the most unfavorable location of lining structure. When water pressures act on left arch waist, left wall, and left arch foot, the internal forces and displacements are generally in a biased state, with a distribution pattern of larger on left side and smaller on right side. The responses of internal force and displacement at action locations of water pressure are the most rapid and maximum, and the influence degree of water pressure

[1]Eng., Department of Technical Contract, Chongqing Yuxiang Double-line Expressway Co. Ltd., No. 66 Yinshan Road, Yubei District, Chongqing, China, e-mail: 874098896@qq.com, ORCID: 0009-0009-0453-0926
[2]Eng., Institute of Tunnel and Underground Engineering, China Merchants Chongqing Communications Technology Research & Design Institute Co., Ltd., No. 33 Xuefu Avenue, Nan'an District, Chongqing, China, e-mail: 228936546@qq.com, ORCID: 0009-0000-5261-5304
[3]Eng., None, Chongqing Yuxiang Double-line Expressway Co. Ltd., No. 66 Yinshan Road, Yubei District, Chongqing, China, e-mail: 470875479@qq.com, ORCID: 0009-0002-9259-4194
[4]Prof., Institute of Tunnel and Underground Engineering, China Merchants Chongqing Communications Technology Research & Design Institute Co., Ltd., No. 33 Xuefu Avenue, Nan'an District, Chongqing, China, e-mail: huxuebin@cmhk.com, ORCID: 0009-0007-8870-0608
[5]Prof., Department of Technical Contract, Chongqing Yuxiang Double-line Expressway Co. Ltd., No. 66 Yinshan Road, Yubei District, Chongqing, China, e-mail: 3037633434@qq.com, ORCID: 0009-0004-5787-4486
[6]Prof., DSc., Institute of Tunnel and Underground Engineering, China Merchants Chongqing Communications Technology Research & Design Institute Co., Ltd., No. 33 Xuefu Avenue, Nan'an District, Chongqing, China, e-mail: lightcheng@126.com
[7]DSc., Eng., Department of Technical Contract, Chongqing Yuxiang Double-line Expressway Co. Ltd., No. 66 Yinshan Road, Yubei District, Chongqing, China, e-mail: sirixian@126.com, ORCID: 0000-0002-6008-466X

gradually decreases with increasing distance. Overall, the farther away from the action locations of water pressure, the greater the safety factor of tunnel structure.

Keywords: high water pressure, internal force, karst tunnel, lining structure, stability analysis

1. Introduction

Karst geology is widely distributed in China, accounting for about one-third of the total land area, especially in the Southwest region [1–4]. With the rapid development of China's transportation infrastructure, the number of tunnels built in karst areas is increasing day by day. However, there are many cracks and dissolved pipelines in the rock mass in karst area. Due to the influence of surface rainfall infiltration and groundwater seepage, many water-enriched karst tunnels have experienced cracking of lining structure, water leakage, and water inrush disasters, etc., seriously affecting the operation safety and service life of tunnels [5–7]. According to the controlled drainage principle of "to block the main, limited emissions" [8], in the operation of karst tunnels, the complex water pressure distribution phenomena are often encountered behind the lining structure. The presence of high water pressure poses a huge threat and challenge to the stability of surrounding rock and the safety of tunnel lining structure. Therefore, it is very necessary and meaningful to investigate the force and deformation properties and the stability of tunnel lining structure subjected to water pressures with the different conditions.

Many scholars at home and abroad have conducted relevant research on tunnel diseases in karst areas and achieved a series of results. Li et al. [9] studied the influence of spatial distribution characteristics of karst caves on the stress characteristics of highway tunnel lining structure in karst areas based on indoor tunnel model experiments. Wang [10] adopted Flac3D software to simulate the displacement characteristics of tunnel lining structure with the high-pressure water filled karst caves on the left side, and compared the numerical results with on-site monitoring data. Fan et al. [11] conducted the mechanical response model tests on the lining structure of karst tunnels with rich water pipelines, and the internal force characteristics of the tunnel lining structure under the actions of different cavity positions and water head heights were studied. And the influences of cavity diameter, cavity position and water head height on the lining structure were investigated. Ouyang et al. [12] analyzed the change rule of surrounding rock displacement and tunnel structure internal force with time during the construction of the low mountain ridge tunnel based on the Xishan Tunnel Project. Huang et al. [13] analyzed the hydraulic pressure resistance and damage process of the tunnel grouting body in karst zone by using RFPA software. Shen et al. [14] reviewed the historical diseases and analyzed the reasons of the structural diseases based on the Nanshibi Tunnel project. And the comprehensive measures were adopted to resolve the tunnel diseases in the karst zone. Arjnoi et al. [15] studied the distribution patterns of water pressure on lining structure and the internal force under the different drainage methods, and it was found that the full drainage can significantly reduce the stress of the tunnel lining structure. Zhao et al. [16] and Li et al. [17] also studied the water pressure distribution of lining structure under the different forms of waterproofing and drainage structures, and proposed an optimized waterproofing

and drainage structure which is suitable for water-enriched tunnels. Li et al. [18] adopted Midas/GTS software to establish the three-dimensional karst tunnel model to study the stress characteristics of lining structure under the actions of karst caves with different azimuth angles. And the influence laws of the distance between karst cave and tunnel, and the azimuth angle of karst cave on the stress of tunnel lining structure were studied. Mo et al. [19] and Song et al. [20] studied the influences of hidden water-enriched cavity on the internal force and displacement of lining structure through numerical calculations and model experiments. The existing researches mainly focus on the interaction mechanism between the karst caves and the surrounding rock and tunnel lining structure, and the stability analysis of lining structure of karst tunnels under the action of water pressure under a certain working condition. However, the size and water pressure magnitude of karst cave, as well as its distribution relationship with tunnels, are very complex. The internal force and deformation properties of tunnel lining structure subjected to water pressures with the different action conditions have still been unclear. Therefore, in this paper, based on FLAC3D software, according to the geological condition of actual on-site karst tunnel engineering, numerous tunnel models subjected to water pressures with different action conditions were established. The influences of the magnitude, range, and action location of local water pressures on the internal force and deformation properties, and stability of tunnel lining structure were studied. Firstly, the distribution laws of internal force including bending moment and axial force were obtained. Then, the deformation properties of horizontal displacements and vertical displacements were analyzed. Next, the safety factors of tunnel lining structure at different locations were investigated. The research results could provide reference for analyzing and evaluating the stability of tunnel lining structures in similar karst area.

2. Numerical simulation models

2.1. Model building

According to hydraulic principle, the karst terrain and water level differences are important factors affecting the distribution of water pressure acting on tunnel lining, including the size and range of potential karst caves, and the connection degree with other water source paths. If the karst cave behind the lining is connected to the surface, the natural precipitation will increase the water pressure inside the cave, thereby exerting higher pressure on surrounding rock and lining. Moreover, during the water accumulated process, the sand and stones carried by rainwater gradually accumulate between cave and lining during the. The long-term accumulation may block the flow pipeline, weaken the diffusion of water in the karst cave after rainfall and ultimately completely block flow pipeline. As a result, the accumulated water in the karst cave can be regarded as a local concentrated water head pressure directly acting on the lining. In this paper, the main purpose is to investigate the mechanical responses of lining structures under the specific high water pressure environments. Therefore, the influences of water flow in rock cracks are not considered; instead, the total effect of external water pressure is assumed to apply to the local lining structure, namely the extreme adverse working condition.

It is assumed that the water pressure is only formed inside karst cave, and the water pressure is simulated by applying surface forces on the lining surface. When balancing the initial geo-stress, only self-weight stress is considered, ignoring the influence of tectonic stress. And the drainage system is not installed to simulate the situation where the drainage pipeline is completely blocked. In this work, based on FLAC3D Finite element difference software, the numerical simulation models are established according to the karst concentration section of Pengshui Tunnel, namely YK156+290~YK156+350 section. As shown in Fig. 1, the tunnel excavation span is 12.82 m, and the height and burial depth of tunnel are 10.25 m and 200 m, respectively. The S5ay composite lining structure is adopted as in Fig. 2. The existing theoretical analysis results [21] indicate that the stress state within a certain range near the tunnel will be affected by tunnel excavation, while the surrounding rock outside a certain range will not be affected, and the influencing range is generally taken as 3–5 times the tunnel excavation width. Therefore, the total length, width and height of calculation model are set as 60 m, 90 m and 100 m, respectively. Because the tunnel is buried at a depth of 200 m, the remaining height of rock is converted into a uniformly distributed loading with a value of 3360 kPa, which is applied to the top surface of calculation model.

As shown in Fig. 1, the grid element sizes of tunnel lining and rock layer are set as 1 m and 2 m, respectively. And the front, back, left, and right surfaces of the numerical simulation model are set as the normal constraint boundaries. The bottom surface is with fixed boundary, and the top surface is free boundary. Besides, due to ignoring the influence of groundwater seepage, the seepage conditions are not considered as for all the boundaries.

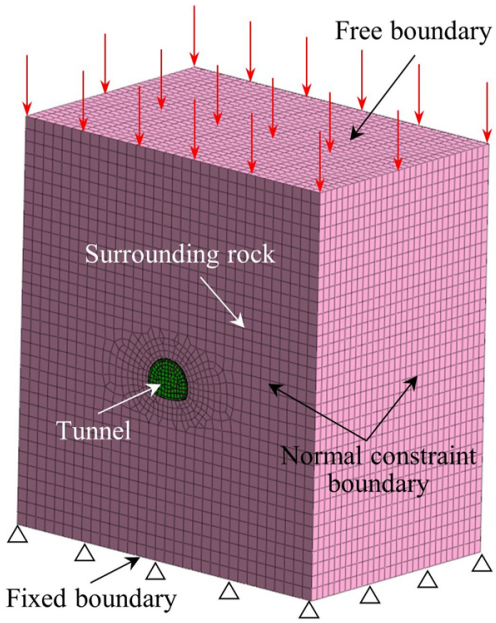

Fig. 1. Numerical calculation model

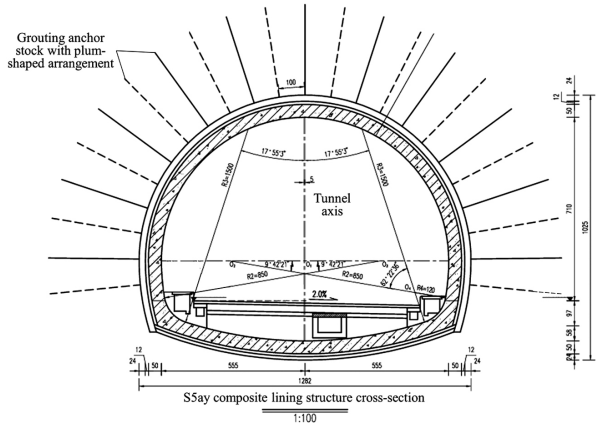

Fig. 2. Section schematic diagram of tunnel lining structure

2.2. Material parameters

In numerical simulations of this paper, the Mohr-Coulomb strength criterion is used to describe the response characteristics of stress deformation for the surrounding rock. The secondary lining structure is described by adopting the solid elements that comply with the elastic yield criterion. The karst cave part is represented by an empty model. And the shell elements are adopted to simulate the initial support of tunnel. In the design of initial support structures, the bearing capacity of the steel mesh is relatively small, and its main function is to provide an attachment base for shotcrete. Therefore, this is usually not considered in the numerical simulation calculation process. But as for the effect of the steel frame in the initial support structure, the "substitution stiffness method" is usually adopted [22, 23], which is achieved by converting the deformation resistance of the steel arch into the equivalent stiffness of shotcrete. According to the "Design Specification for Highway Tunnels" (JTG3370.1-2018) [24] and the actual engineering geological report, the related parameters of surrounding rock and support structure have been determined as given in Table 1.

Table 1. Material parameters in numerical simulations

Parameters	**Elastic modulus /GPa**	**Bulk density /(kN/m^3)**	**Poisson's ratio**	**Cohesive force /MPa**	**Internal friction angle /°**	**Thickness /m**
Surrounding rock	2.0	20	0.4	0.2	28	–
Initial liner	26.5	24.5	0.2	–	–	0.25
Second lining	32.5	26	0.2	–	–	0.5

2.3. Numerical simulation scheme

In numerical simulations, the research focus of this paper is to analyze the effects of local water pressure behind tunnel on the internal force and deformation characteristics of the secondary lining structure. So, the tunnel section at the action range center of water pressure in karst cave is selected as the monitoring section. As shown in Fig. 3, the corresponding points for monitoring the deformation and stress characteristic of lining structure are set, specifically including tunnel vault, arch waist, side wall, arch foot and inverted arch. In this paper, the influences of the different locations and sizes of karst caves, and water pressures on the tunnel lining structure will be studied. As given in Table 2, the locations of karst caves are selected at the tunnel vault, left arch waist, left side wall, and left arch foot, respectively. The action range of water pressure is 1 m, 2 m, and 3 m in diameter, respectively. The water head heights are 20 m, 40 m, 80 m, 120 m, 160 m, and 200 m respectively, and the corresponding water loadings on lining structure are 0.2 MPa, 0.4 MPa, 0.8 MPa, 1.2 MPa, 1.6 MPa, and 2.0 MPa, respectively.

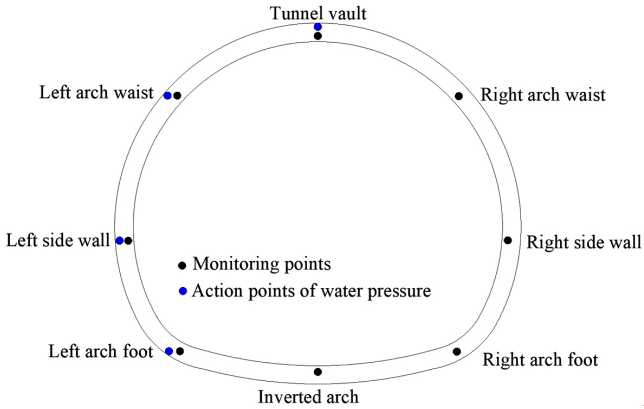

Fig. 3. Layout schematic diagram of action points of water pressure and monitoring points

Table 2. Calculation scheme parameters in numerical simulations

Action location of water pressure	**Cave diameter /m**	**Water pressure value /MPa**					
Tunnel vault	1	0.2	0.4	0.8	1.2	1.6	2.0
	2	0.2	0.4	0.8	1.2	1.6	2.0
	3	0.2	0.4	0.8	1.2	1.6	2.0
Left arch waist	3	2.0					
Left side wall							
Left arch foot							

3. Effects of local water pressure position on the force and deformation characteristic of tunnel lining structure under different pressure parameters

FLAC3D software cannot directly output the bending moment, internal force, and safety factor values for the numerical calculation model. So, in this paper, the lining structure is divided into the inner and outer layer elements with same thickness, and then the required internal force values can be calculated by extracting the centroid stress and corresponding coordinates of the above-mentioned two-layer elements through the Fish function [25]. Assuming the coordinates of the centroids of inner and outer layer elements are (x_1, y_1) and (x_2, y_2), respectively. And the angle between the vertical plane and the lining section passing through the element centroid, α, is as follows:

$$\alpha = \arctan[(x_2 - x_1)/(y_2 - y_1)] \tag{3.1}$$

As shown in Fig. 4, the normal stress corresponding to the element centroid can be calculated as follows:

$$\sigma_n = \sigma_x \cos^2\theta + \sigma_y \sin^2\theta - \tau_{xy} \sin 2\theta \tag{3.2}$$

where σ_n is the normal stress corresponding to the element centroid; σ_x, σ_y, and τ_{xy} are the stress components corresponding to the element centroid; θ is the angle between stress component σ_x and the outer normal of cross-section, which in counterclockwise is as positive, namely $\theta = -\alpha$.

Stresses at the edges of the inner and outer elements of the tunnel lining structure can be calculated according to the method of linear interpolation. They are as follows:

$$\sigma_1 = 0.5(\sigma_{n1} + \sigma_{n2}) + (\sigma_{n1} - \sigma_{n2}) \tag{3.3}$$

$$\sigma_2 = 0.5(\sigma_{n1} + \sigma_{n2}) - (\sigma_{n1} - \sigma_{n2}) \tag{3.4}$$

where σ_1 and σ_2 are the stress of outer element and inner element of tunnel lining structure, respectively. σ_{n1} and σ_{n2} are the normal stresses corresponding to the outer element centroid and inner element centroid of tunnel lining structure, respectively; So, according to the principles of material mechanics, the bending moment M and axial force N on the cross section can be calculated as follows:

$$M = bh^2(\sigma_1 - \sigma_2)/12 \tag{3.5}$$

$$N = bh(\sigma_1 + \sigma_2)/2 \tag{3.6}$$

where b and h are the width and thickness of the cross-section, respectively, and b is generally taken as 1 m.

The safety factor of the lining structure can be obtained by combining the above-mentioned internal force values calculated by formulas (3.1)–(3.6). According to the "Design Specification for Highway Tunnels" (JTG3370.1-2018) [24], the safety factor K of the tensile or compressive strength of the cross section is determined by the ratio of the ultimate bearing capacity N_u to the actual internal force N of the component, which is given as follows:

$$K = N_u/N \geq [K] \tag{3.7}$$

where K and $[K]$ are the safety factor and allowable safety factor of the lining structure, respectively. N_u is the ultimate bearing capacity of the lining structure component. When the eccentricity $e = M/N \leq 0.2h$, the material failure is mainly controlled by the compressive strength criterion, and its ultimate bearing capacity is calculated as follows:

$$N_u = \phi \alpha R_c b h \tag{3.8}$$

When the eccentricity $e = M/N \geq 0.2h$, the material failure is mainly controlled by the tensile strength criterion, and its ultimate bearing capacity is calculated as follows:

$$N_u = \phi 1.75 R_t b h/(6e/h - 1) \tag{3.9}$$

where ϕ is the longitudinal coefficient of component, and $\phi = 1$ is as for tunnel lining. R_c and R_t are the ultimate compressive and tensile strengths of concrete, respectively. α is the eccentricity influence coefficient of axial force, which can be calculated as follows:

$$\alpha = 1 - 0.648(e/h) - 12.569(e/h)^2 + 15.444(e/h)^3 \tag{3.10}$$

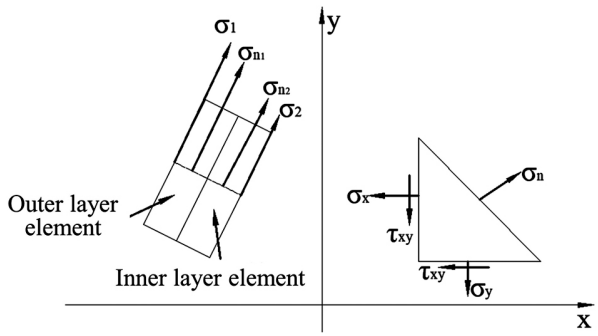

Fig. 4. Schematic diagram for calculating the cross-sectional normal stress

3.1. Effects of local water pressure magnitude and its action range

To investigate the effects of local water pressure magnitude and its action range on the internal force and deformation characteristics of tunnel lining structure, the action position of water pressure is fixed at tunnel vault. And the internal force including bending moment and axial force, horizontal and vertical displacements, and safety factor at different positions of lining structures were analyzed.

3.1.1. Internal force analysis of tunnel lining structure

(1) Bending moment

Figure 5 shows the relationship curves of bending moment of lining structure with water pressure under the different cave diameters. The negative and positive bending moments represent the tension effect on the outer and inner sides of lining structure, respectively. Under

the action of water pressure in tunnel vault, the bending moment values of monitoring points on both sides of lining structure are symmetrically distributed. When the cave diameter is 1 m and the water pressure is 0.2 MPa, the maximum negative bending moment value appears at the arch foot of tunnel lining structure. This indicates that the lining structure is subjected to external tension, with a maximum negative bending moment value of 70.84 kN·m. Moreover, the maximum positive bending moment value appears at the inverted arch, with a maximum positive bending moment value of 45.26 kN·m, which indicates that the lining structure at this position exhibits internal tension. As for different cave diameters, when the water pressure acts on the tunnel vault, the bending moment of tunnel vault changes most significantly compared to other locations, and increases with the increase of water pressure. And there is a significant increase in growth rate when the water pressures are 1.2–1.6 MPa. For example, as for the karst cave with diameters of 1 m and 3 m, when the water pressure increases from 0.2 MPa to 2 MPa, the bending moments of tunnel vault increases from 30.52 kN·m to 193.87 kN·m and from 58.64 kN·m to 340.27 kN·m, with an increase of 163.35 kN·m and 281.63 kN·m, respectively. This indicates that the larger the action range of karst cave on tunnel vault, the more adverse the impact on the lining vault. What's more, the bending moment values at other locations except tunnel vault almost show the linear variation relationships with water pressure. And the bending moment values at arch waist changes more significantly compared with those at side wall, arch foot and inverted arch of tunnel. When the water pressure and cave diameter are relatively small, the bending moments at arch waist are positive values, and they gradually convert negative values and further increase with the increase of water pressure and cave diameter. This is mainly because the arch waist is relatively close to the tunnel vault and is greatly affected by the water pressure in karst cave. On the contrary, the variation of bending moment values at side wall, arch foot and inverted arch of tunnel is relatively slight. This indicates that the influences of water pressure at tunnel vault is relatively small due to the long distance. In all, when there are karst caves in the tunnel vault, it is necessary to consider strengthening protective measures for lining structure not only at tunnel vault but also at arch waist.

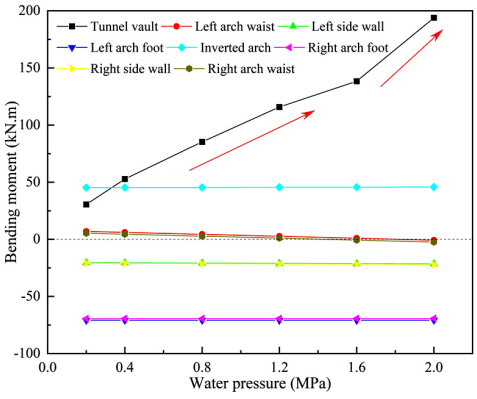

(a)

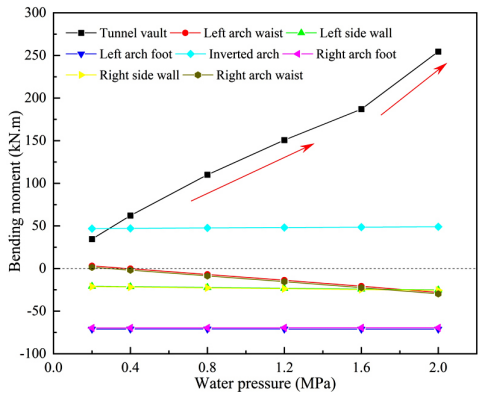

(b)

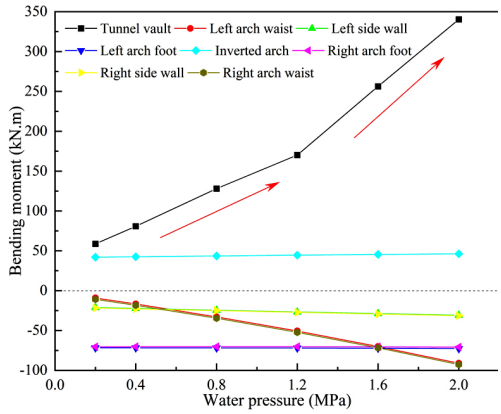

(c)

Fig. 5. Relationship curves of bending moment of lining structure with water pressure under the different cave diameters of: (a) 1 m; (b) 2 m; (c) 3 m

Figure 6 shows the bending moment values at different positions of tunnel lining structure under the different cave diameters. It can be seen that the bending moment values of tunnel lining structure except invert arch increase to varying degrees with the increase of action range of karst cave. For example, when the cave diameter increases from 1 m to 3 m under the water pressure of 0.4 MPa at tunnel vault, the bending moment values of tunnel vault, left arch waist, left side wall and left arch foot increase by 53.1%, –376.7%, 8.3% and 12%, respectively. This is mainly because a larger range of water pressure will bring greater load to the lining results, resulting in greater bending moments. Besides, it can also be seen that due to closer to the action location of water pressure, the variations of bending moments at tunnel vault and arch waist are more obvious than those at other locations.

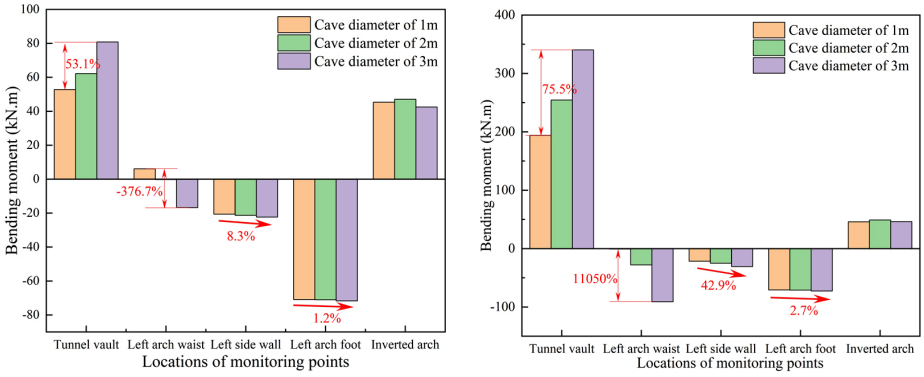

(a) (b)

Fig. 6. Bending moment values at different positions of tunnel lining structure under the different cave diameters: (a) Water pressure of 0.4 MPa; (b) Water pressure of 2.0 MPa

(2) Axial force

Figure 7 shows the relationship curves of axial force of lining structure with water pressure under the different cave diameters. Under the action of water pressure in tunnel vault, the distribution patterns and change trends of axial force of lining structure are similar to the bending moment. The axial force values of lining structure show a symmetrical distribution pattern and are all negative, indicating that the lining structure is in a compressed state. This is beneficial to the concrete structure that mainly bears compressive capacity to a certain extent. As for the different karst cave diameters, the axial forces of tunnel vault increase significantly with the increase of water pressure; especially when the cave diameter is 3 m, its variation trend is an exponential increase, with an increase rate of 204% as the water pressure increases from 0.2 MPa to 2 MPa. Besides, only when the action of water pressure is small, such as cave diameter of 1 m and water pressure of 0.2 MPa, the maximum axial force value appears near the side wall of tunnel lining structure, with a maximum axial force value of –1451.60 kN. Under other action conditions of water pressure, the maximum axial forces all occurs at tunnel vault. Except for the change in axial force at tunnel vault, the change in axial force at arch waist is also more significant, and almost increases linearly with the increasing water pressure. When the water pressure increases from 0.2 MPa to 2 MPa at cave diameter of 3 m, the axial force at arch waist increases from –856.54 kN to –1928.16 kN, with a growth rate of 125%. The above phenomenon is mainly caused by different distances from the action location of water pressure, and the farther the distance, the less affected the water pressure is. For example, the axial forces at left arch foot and inverted arch only change 58.45 kN and 61.68 kN as for the water pressures from 0.2 MPa to 2 MPa at cave diameter of 3 m, with a variation rate of 5% and 20%, respectively. As shown in Fig. 8, as for the different water pressures, the axial force values of tunnel lining structure except for inverted arch all increase with the action range of karst cave. The order of growth rates of axial force is tunnel vault, arch waist, side wall, and arch foot, in sequence. For example, the growth rates for tunnel vault, arch waist, side wall, and arch foot under the action of water pressure of 2 MPa, are 133.39%, 71.4%, 20.7% and 5.3%, respectively.

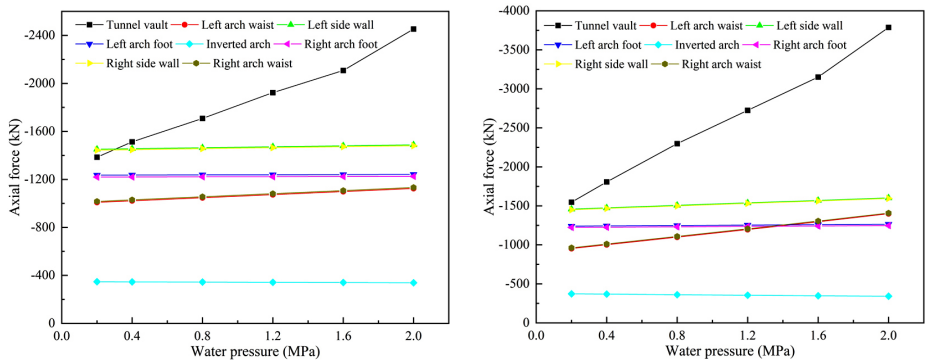

(a) (b)

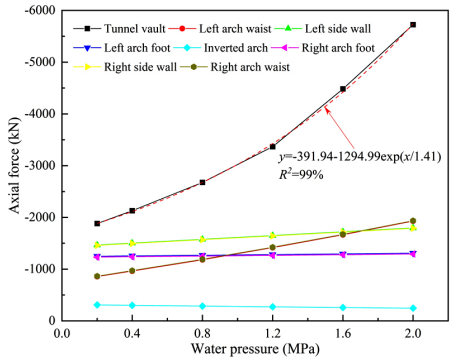

(c)

Fig. 7. Relationship curves of axial force of lining structure with water pressure under the different cave diameters of: (a) 1 m; (b) 2 m; (c) 3 m

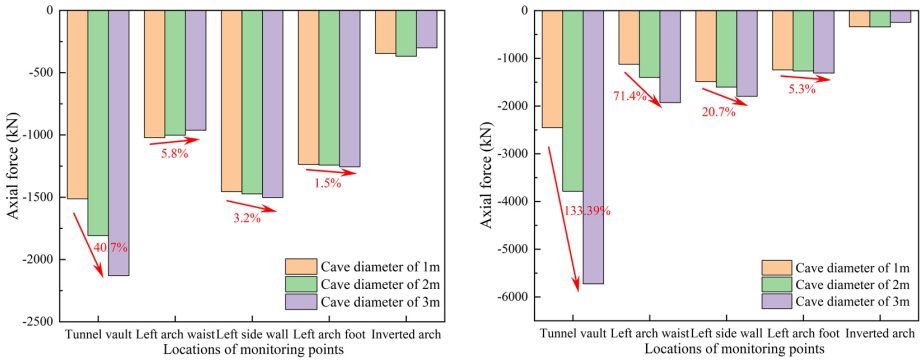

(a) (b)

Fig. 8. Axial force values at different positions of tunnel lining structure under the different cave diameters: (a) Water pressure of 0.4 MPa; (b) Water pressure of 2.0 MPa

3.1.2. Displacement analysis of tunnel lining structure

(1) Horizontal displacement

Figure 9 shows the cloud maps of horizontal displacement of lining structure under the action of different water pressures when the karst cave diameter is 3 m. Moreover, as for the different water pressure magnitudes and its action range, the horizontal displacements at different positions of lining structures were extracted. It can be seen that the horizontal displacement of lining structure also shows a symmetrical distribution trend when the water pressure acts on the tunnel vault. The left and right sides of tunnel lining will experience horizontal deformation to the left and horizontal deformation to the right, respectively. And the area near the tunnel arch will experience inward compression deformation. According to the continuum theory and elastic-plastic theory, the equivalent region of horizontal displacement

at the upper part of lining will undergo deformation in synergy with each other. During this deformation process, the surrounding rock on the left upper part of tunnel vault and the right part of arch waist will undergo rightward displacement, forming a diagonal displacement that intersects with the action point of water pressure at tunnel vault and expands outward. This indicates that during the descent of tunnel vault under the action of water pressure at tunnel vault, the lining structure at arch waist and arch foot will expand outward, while the maximum horizontal displacement occurs at arch waist. Fig. 10 shows the horizontal displacements at different positions under the different cave diameters and their relationships with water pressure. It can be seen from Fig. 10 that under the same action range of water pressure namely cave diameter, the horizontal displacement values at side wall and arch foot of tunnel all increase linearly with the increase of water pressure magnitude. And the horizontal displacement values at side wall are greater than those at arch foot. For example, under the action of water pressure with a cave diameter of 3 m, when the water pressure changes from 0.2 MPa to 2.0 MPa, the horizontal displacement values at right side wall and right arch foot increase from –0.004 mm to 0.389 mm and from 0.002 mm to 0.073 mm, respectively. And as the cave diameter increases, the horizontal displacement values of tunnel lining structure also increase significantly. When the cave diameter increases from 1 m to 3 m for the water pressure of 2 MPa, the horizontal displacement values at left and right side walls, left and right arch foots, increase by 781% and 780%, 840% and 851%, respectively. The above phenomena indicate that the water pressure magnitude and its action range both have a significant impact on the deformation of lining structure. Besides, due to the distance between the inverted arch and the action position of water pressure at tunnel vault, it can be observed from the cloud maps that the deformation at inverted arch is relatively small.

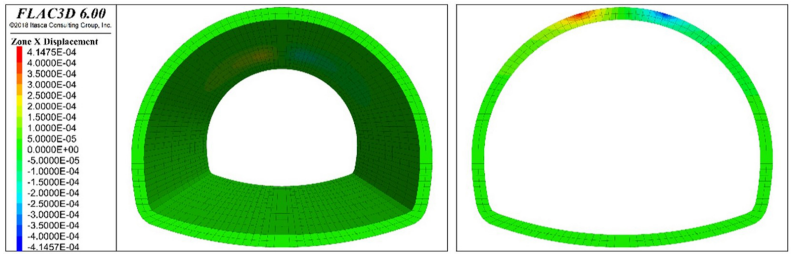

(a) Water pressure 0.2 Mpa

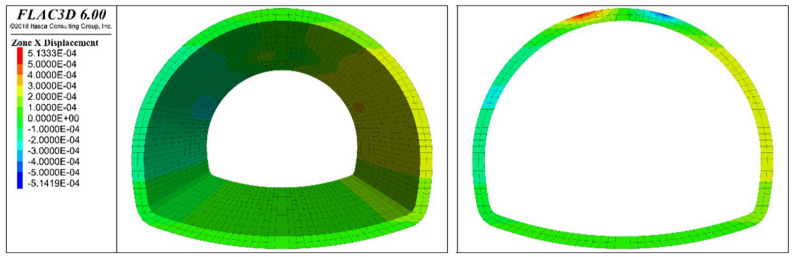

(b) Water pressure 1.2 Mpa

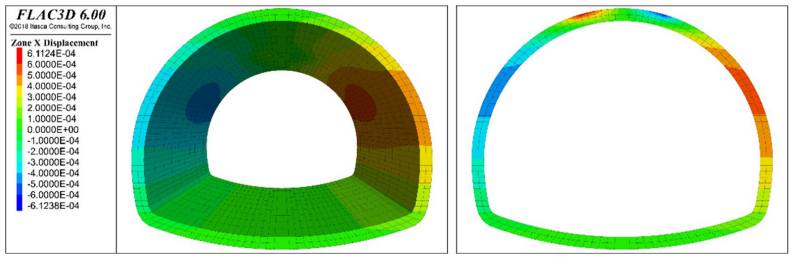

(c) Water pressure 2.0 Mpa

Fig. 9. Cloud maps of horizontal displacement of lining structure under the action of different water pressures for the cave diameter of 3 m: (a) 0.2 MPa; (b) 1.2 MPa; (c) 2.0 MPa

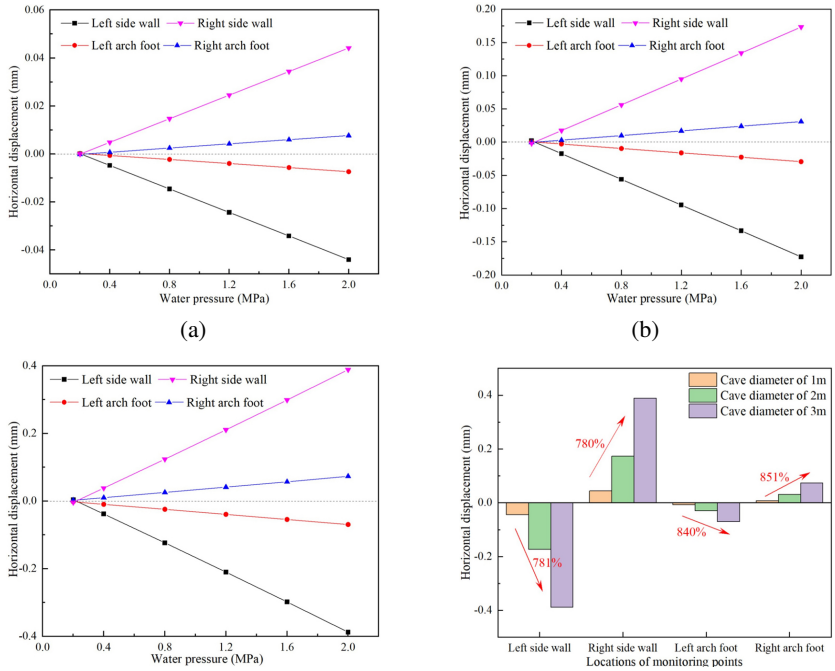

Fig. 10. Horizontal displacements at different positions under the different cave diameters and their relationships with water pressure: (a) Cave diameters of 1 m; (b) Cave diameters of 2 m; (c) Cave diameters of 3 m; (d) Horizontal displacements at different positions for water pressure 2 MPa

(2) Vertical displacement

Figure 11 shows the cloud maps of vertical displacement of lining structure under the action of different water pressures when the karst cave diameter is 3 m. And Fig. 12 shows the vertical displacements at different positions under the different cave diameters and their relationships with water pressure. It can be seen Fig. 11 and Fig. 12 that when the tunnel

vault is subjected to water pressure load, the vertical displacement values of lining structure are negative, indicating that the tunnel lining structure are deformed downwards. And the tunnel vault will suffer from the maximum settlement displacement, followed by arch waist and inverted arch, as show in Fig. 12. For example, when the action range of water pressure is 3 m, the maximum settlement displacement at tunnel vault is 3.96 mm, which is 6.32 times than that at the cave diameter of 1 m. Besides, the vertical displacement values at different position of tunnel structure also almost increase linearly with the increasing water pressure magnitude. When the vertical displacement at tunnel vault reaches its peak, the monitoring part of lining structure has been damaged. What's more, the vertical deformation of tunnel is mainly concentrated at vault, and the left and right arch waists. As the magnitude of water pressure at tunnel vault and its action range increase, the deformation area of lining structure shows a trend of spreading from top to bottom. This indicates that the deformation effect caused by the water pressure at tunnel vault is not limited to the area near vault, but gradually affects the entire lining structure and even the arch foot, as the action range of water pressure increases.

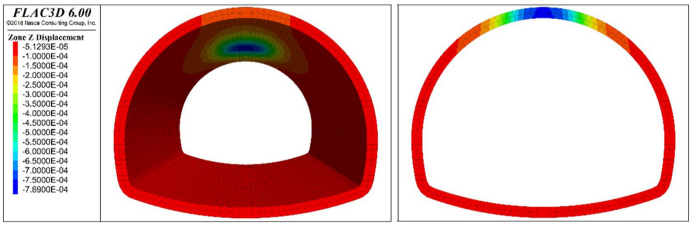

(a) Water pressure 0.2 Mpa

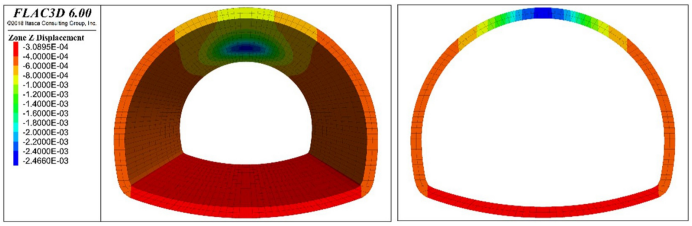

(b) Water pressure 1.2 Mpa

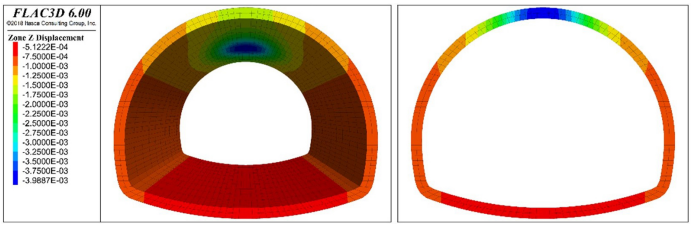

(c) Water pressure 2.0 Mpa

Fig. 11. Cloud maps of vertical displacement of lining structure under the action of different water pressures for the cave diameter of 3 m: (a) 0.2 MPa; (b) 1.2 MPa; (c) 2.0 MPa

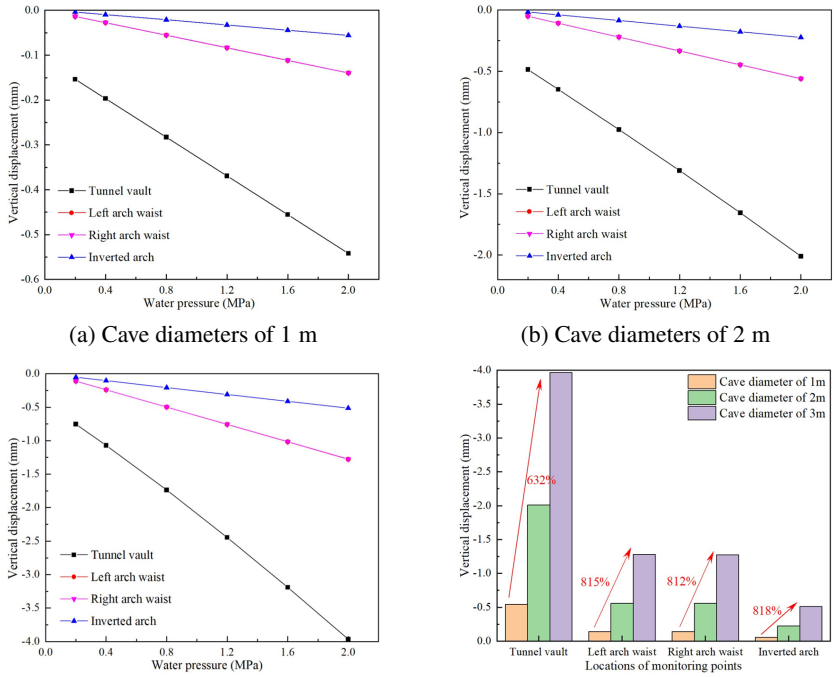

(a) Cave diameters of 1 m

(b) Cave diameters of 2 m

(c) Cave diameters of 3 m

(d) Vertical displacements at different positions for water pressure 2 MPa

Fig. 12. Vertical displacements at different positions under the different cave diameters and their relationships with water pressure: (a) Cave diameters of 1 m; (b) Cave diameters of 2 m; (c) Cave diameters of 3 m; (d) Vertical displacements at different positions for water pressure 2 MPa

3.1.3. Safety factor of tunnel lining structure

Figure 13 shows the relationship curves of safety factor of lining structure with water pressure under the different cave diameters. When the tunnel vault is subjected to a water loading with a diameter of 1 m and pressure of 0.2 MPa, the safety factors at side walls are the smallest, and the safety factor values at left and right side-walls are 9.14 and 9.18, respectively. The safety factor at tunnel vault is maximum, reaching 14.20. With the increase of water pressure, the change of safety factor at tunnel vault is most significant, and decreases exponentially to 4.55 when the water pressure increases to 2 MPa, which is the minimum safety factor under the action of water pressures with different magnitudes. And the safety factor values of other monitoring points change relatively little with the increasing water pressure and show an almost linear slow decreasing trend. At this time, the safety factor values of all monitoring points are greater than the safety factor 2.4 for compression resistance and the safety factor 3.6 for tensile resistance in the tunnel design specifications, indicating that the tunnel lining structure is still within the safe range of concrete design. With the further increase of water pressure, the decreasing changes of safety factors for most monitoring points become more significant. The changes of safety factors at arch waist and inverted arch gradually show

an exponential significant decrease trend when the water pressure increases to 3 MPa. However, the change in safety factor at tunnel arch foot is still very small, which corresponds to the fact that the internal force at arch foot is less affected by the water pressure at tunnel vault. Specifically, as for the action range of water pressure with a cave diameter of 2 m, the safety factor at tunnel vault is 3.62 when the water pressure is 1.6 MPa, approaching the safety factor of 3.6 for tensile. This indicates that the tunnel lining structure vault has developed from a small eccentric compression state to a large eccentric tension state. As the water pressure further increases to 2.0 MPa, the safety factor at tunnel vault has been reduced to 2.18, which is lower than critical value of 3.6. On the other hand, as for the action range of water pressure with a cave diameter of 3 m, the safety factor at tunnel vault is reduced to 3.80 at 1.2 MPa, and the lining structure is in a large eccentric tensile state. And the closer the other monitoring points are to the tunnel vault, the lower the safety factor value; and the safety factor at inverted arch also decreases rapidly, with a minimum value of 6.58. The above phenomena indicate that the water pressure magnitude has a significant impact on the safety factors of monitoring points within the action range of water pressure. And the action range of water pressure will cause a sudden change and decrease in the safety factor of monitoring points in advance.

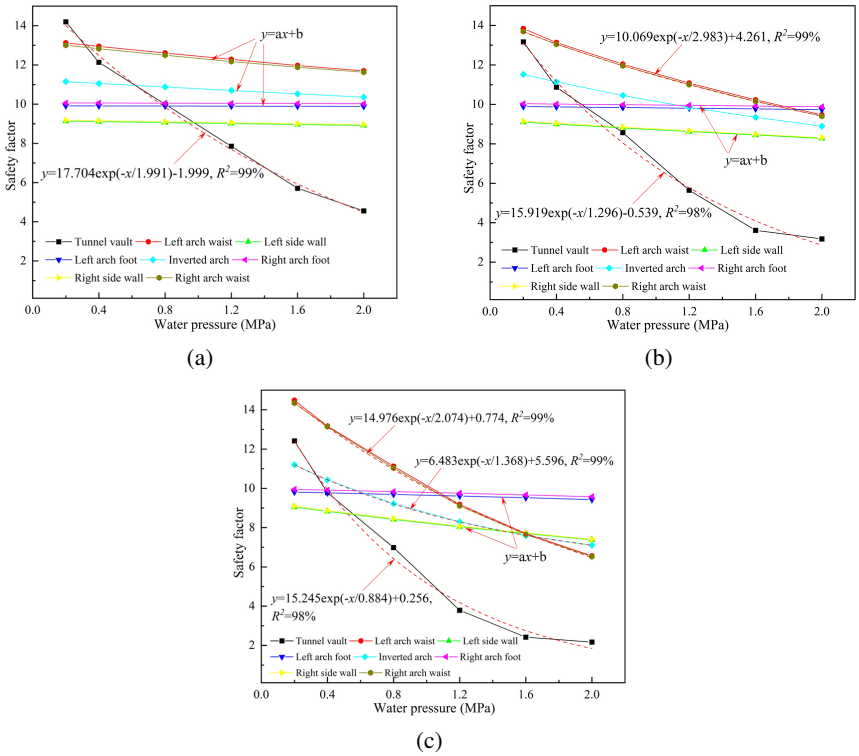

Fig. 13. Relationship curves of safety factor of lining structure with water pressure under different cave diameters: (a) 1 m; (b) 2 m; (c) 3 m

3.2. Effects of local water pressure action position

(1) Internal force

Figure 14 shows the effect of water pressure at different locations on the bending moment and axial force of lining structures at different locations, where the water pressure and its action range are 2 MPa and 3 m, respectively. On the one hand, when the water pressure loading acts on the tunnel vault, the bending moment values for the monitoring point on both sides of tunnel lining structure are symmetrically distributed. But when the water pressure loading acts on the left arch waist, left wall, and left arch foot, the bending moment values are not symmetrically distributed and is in a state of eccentric compression. And the bending moment values at the action location of water pressure are most significant, and generally show an internal tensile state for the tunnel lining structure. On the contrary, the bending moment values away from the action location of water pressure are relatively small, most of which are negative bending moments, indicating that the exterior of lining structure are subjected to a certain degree of tensile action. For example, when the water pressure loadings act on the tunnel vault, left arch waist, left wall, and left arch foot, the bending moment values at above locations are maximum, reaching 340.27 kN·m, 439.89 kN·m, 390.61 kN·m, and 101.63 kN·m, respectively. And the bending moment values at other locations especially when the water pressures act on the tunnel vault, left arch waist and left side wall, are relatively small, not exceeding 43% of the maximum bending moment values. As shown in Fig. 14(b), the variation laws of axial force are similar to that of bending moment. The response of axial force of tunnel lining structure at the action location of water pressure is the most rapid, leading to the maximum axial force values. The axial force values at other locations are less affected by water pressure, and the influence degree gradually decreases with increasing distance. When the water pressure loadings act on the tunnel vault, left arch waist, left wall, and left arch foot, the axial force values at above locations are maximum, reaching –5725.45 kN, –5581.34 kN, –5429.18 kN, and –5184.42 kN, respectively. And the axial force values at other locations shall not exceed 41% of their maximum axial force values.

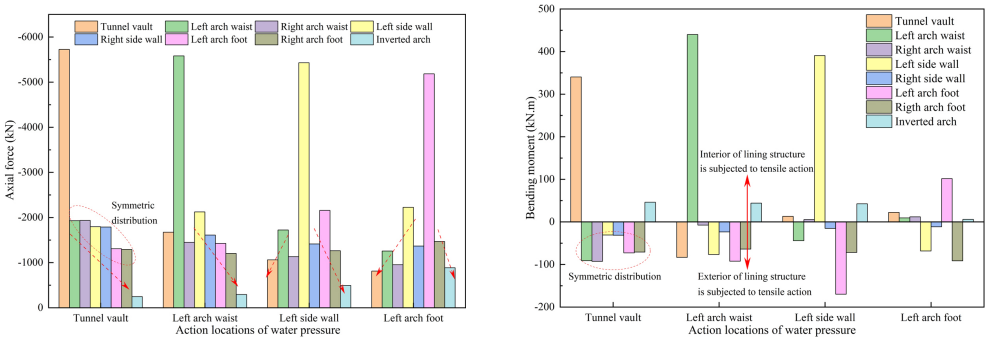

Fig. 14. The effect of action locations of water pressure on the internal forces of lining structures at different locations: (a) Bending moment; (b) Axial force

(2) Deformation displacement

Figure 15 shows the effect of water pressure at different locations on the horizontal displacement and vertical displacement of lining structures at different locations, where the water pressure and its action range are 2 MPa and 3 m, respectively. When the water pressure acts on the tunnel vault, the vault area of lining structure will experience inward compression deformation, which will transfer to the left and right sides. As a result, the left and right arch waists and side walls appear the outward compression deformation, and the horizontal displacement and vertical displacement on both sides of tunnel lining structure are symmetrically distributed. And the maximum displacements occur at the tunnel vault within the action range of water pressure, and are mainly the settlement deformation, namely –3.964 mm. When the water pressure acts on the left arch waist, left side wall and left arch foot, respectively, the displacements on the left side of lining structure are generally greater than those on the right side. The overall deformation of the tunnel lining structure is squeezed to the right side, and the deformation of lining structure is most obvious within the action range of water pressure. Under the action of water pressure at left arch waist and left side wall, the deformations of lining structure are mainly vertical deformation and horizontal displacement, respectively, and the maximum vertical displacement and horizontal displacement reach –3.314 mm and 3.431 mm. However, the influence of the water pressure at arch foot on the deformation change outside the action range of water pressure is less affected, especially as for the vertical displacement.

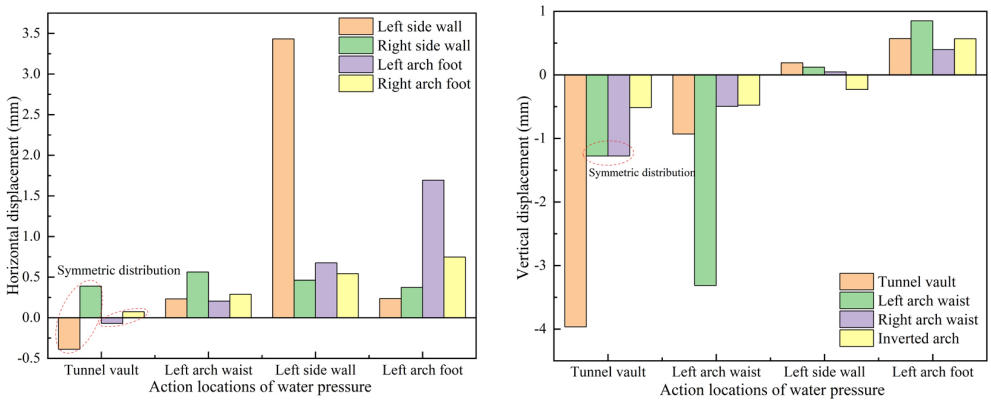

(a) (b)

Fig. 15. The effect of action locations of water pressure on the deformation displacements of lining structures at different locations: (a) Horizontal displacement; (b) Vertical displacement

(3) Safety factor

Figure 16 shows the effect of water pressure at different locations on the safety factor of lining structures at different locations. Under the action of water pressure with a pressure of 2 MPa and cave diameter of 3 m, respectively, the safety factors at the action locations of water pressure are lowest, which are below the critical safety factors for compression resistance and tensile resistance. As for the actions of water pressure at tunnel vault, left arch waist, left side

wall and arch foot, the lowest safety factors are 2.173, 2.106, 2.22 and 2.654, respectively. The safety factors are relatively high in other locations except for the action range of water pressure, which are higher than the critical safety factors, indicating that they are not significantly affected by water pressure. Overall, the farther away from the action location of water pressure, the greater the safety factor of tunnel lining structure.

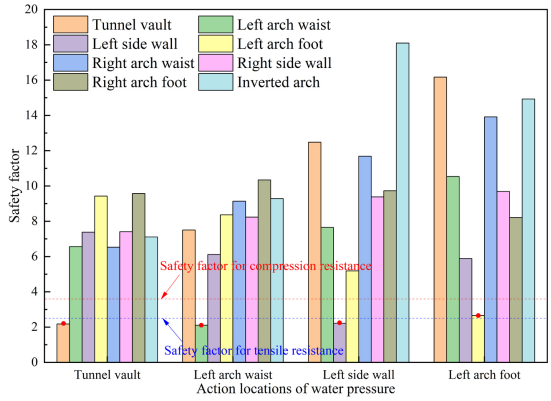

Fig. 16. The effect of action locations of water pressure on the safety factor of lining structures at different locations

4. Conclusions

In this paper, numerous tunnel models subjected to water pressures at different locations were established based on FLAC3D software. And the influences of action location, magnitude and range of water pressure on the internal force and deformation characteristics of tunnel lining structure were investigated. The following main conclusions could be obtained:

1. When water pressure loading acts on tunnel vault, the bending moments and axial forces of tunnel lining structures have the similar and symmetric distribution laws. The maximum values basically occur on tunnel vault and increase significantly with the increase of water pressure and its action range, while the internal force values in other locations have small changes. When water pressure acts on left arch waist, left wall, and left arch foot, the distribution of bending moments and axial forces are in a state of eccentric compression. The internal force responses at action location of water pressure are the most rapid with the occurrence of maximum values, and the influence degree of water pressure on internal forces gradually decreases with increasing distance. As for bending moment values, the interior and exterior of tunnel lining structure are subjected to a certain degree of tensile action at action locations of water pressure and other locations, respectively.
2. When water pressure loading acts on tunnel vault, the horizontal and vertical displacements of lining structure are symmetrically distributed. The maximum displacements occur at tunnel vault and are mainly the settlement deformations. And as the magnitude

and action range of water pressure increase, the displacement values at different locations of tunnel lining structure all show the nearly linear growth trend with different amplitudes. When water pressure acts on left arch waist, left wall, and left arch foot, the displacements on left side of lining structure are generally greater than those on right side due to the rightward squeezing effect of water pressure. The deformations of lining structure within the action range of water pressure are more obvious, which are mainly vertical deformation and horizontal displacements as for the actions of water pressure at left arch waist and left side wall, respectively. And the influence of water pressure at arch foot on deformation change outside the action range of water pressure is less affected, especially as for the vertical displacement.

3. With the increase of water pressure when water pressure acting on tunnel vault, the changes of safety factors near the action location of water pressure are significant with a maximum change on tunnel vault and decrease exponentially; and the above region with significant changes increases with the increasing action range of water pressure. The safety factors away from the action locations of water pressure change relatively little and show an almost linear slow decreasing trend with the increasing water pressure. Overall, the farther away from the action locations of water pressure, the greater the safety factor of tunnel lining structure.

Acknowledgements

This work was supported by the Chongqing Transportation Technology Project (Grant/Award Number: CQJT2022ZC13 and 2022-03).

References

[1] M.H. Jin, X.R. Liu, and Z.L. Zhong, "Study on the mechanical characteristics of the lining structure of the karst tunnel under the action of local high water pressure on the vault", *Chinese Journal of Underground Space and Engineering*, vol. 17, no. 4, pp. 1099–1105, 2021.

[2] M.J. Zhao, J.H. Ao, X.H. Liu, and B. Wang, "Model testing research on influence of karst cave size on stability of surrounding rock masses during tunnel construction", *Chinese Journal of Rock Mechanics and Engineering*, vol. 23, no. 2, pp. 213–217, 2004.

[3] K.R. Hong and H.H. Feng, "Development trends and views of highway tunnels in China over the past decade", *China Journal of Highway and Transport*, vol. 33, no. 12, pp. 62, 2020, doi: 10.19721/j.cnki.1001-7372.2020.12.005.

[4] R.Z. Fei, L.M. Peng, C.L. Zhang, J.Q. Zhang, and P. Zhang, "Mechanical characteristics of twin tunnel underneath construction on existing high-speed railway tunnel", *Archives of Civil Engineering*, vol. 69, no. 1, pp. 403–420, 2023, doi: 10.24425/ace.2023.144180.

[5] J.F. Huang, T. Xie, J.J. Chen, Y.S. Qian, and S. Song, "Influence analysis of karst cavity on tunnel stability", *Construction Technology*, vol. 47, no. 14, pp. 30–33, 2018.

[6] K. Li, "Influence of arch karst cave on surrounding rock deformation of tunnel", *Railway Engineering*, vol. 58, no. 2, pp. 48–50, 2018.

[7] Z.Q. Zhou, et al., "Study on tunnel water inrush mechanism and simulation of seepage failure process", *Rock and Soil Mechanics*, vol. 41, no. 11, pp. 3621–3631, 2020, doi: 10.16285/j.rsm.2020.5131.

[8] Z.X. Jiang, "Interaction between tunnel engineering and water environment", *Chinese Journal of Rock Mechanics and Engineering*, vol. 24, no. 1, pp. 121–127, 2005.

[9] X.G. Li, H.N. Zhi, and F. Peng, "Model test analysis on mechanical characteristics of lining of operating highway tunnel in Karst area", *Highway*, vol. 63, no. 5, pp. 296–301, 2018.

[10] H. Wang, "Research and analysis on deformation of surrounding rock and internal force of lining of Guiyang rail transit tunnel by top karst cave", *Hydrogeology and Engineering Geology*, vol. 37, no. 3, pp. 53–58, 2010.

[11] H.B. Fan, et al., "Mechanical response characteristics of lining structure of pipeline karst tunnels in water-rich areas", *Rock and Soil Mechanics*, vol. 43, no. 7, pp. 1884–1898, 2022, doi: 10.16285/j.rsm.2021.1730.

[12] J. Ouyang, H.J. Wang, L.X. Wu, K.X. Zhang, and X.W. Xue, "Construction monitoring and analysis of low mountain ridge tunnel", *Archives of Civil Engineering*, vol. 70, no. 1, pp. 573–587, 2024, doi: 10.24425/ace.2024.148929.

[13] M.L. Huang, J.C. Li, Z. Yang, Z.E. Zhang, and Y. Song, "Analysis and application of lining resistance to water pressure in tunnel through karst cave", *Applied Sciences*, vol. 12, no. 15, art. no. 7605, 2022, doi: 10.3390/app12157605.

[14] J.J. Shen et al., "Causes of tunnel diseases in a karst stratum and remediation measures: A case study", *Frontiers in Earth Science*, vol. 10, art. no. 882058, 2022, doi: 10.3389/feart.2022.882058.

[15] P. Arjnoi, J.H. Jeong, C.Y. Kim, and K.H. Park, "Effect of drainage conditions on pore water pressure distributions and lining stresses in drained tunnels", *Tunnelling and Underground Space Technology*, vol. 24, no. 4, pp. 376–389, 2009, doi: 10.1016/j.tust.2008.10.006.

[16] D.P. Zhao, H.B. Fan, L.L. Jia, and Y. Song, "Research on waterproofing and drainage optimization scheme for karst tunnel lining in water-rich areas", *Environmental Earth Sciences*, vol. 80, no. 4, art. no. 150, 2021, doi: 10.1007/s12665-021-09466-0.

[17] P.F. Li, H.C. Liu, Y. Zhao, and Z. Li, "A bottom-to-up drainage and water pressure reduction system for railway tunnels", *Tunnelling and Underground Space Technology*, vol. 81, pp. 296–305, 2018, doi: 10.1016/j.tust.2018.07.027.

[18] K. Li, Z. Duan, D.Q. Guo, B. Zeng, and Q. Wang, "Study on influence of different azimuth angles of concealed karst cave on the stress characteristics of tunnel lining structure", *Modern Tunnelling Technology*, vol. 60, pp. 74–85, 2023, doi: 10.13807/j.cnki.mtt.2023.S1.10.

[19] Y.C. Mo, "Study on the Influence of water filling in hidden cavity at the bottom of tunnel on the internal force of secondary lining", *Hydrogeology and Engineering Geology*, vol. 38, no. 5, pp. 31–37, 2011, doi: 10.16030/j.cnki.issn.1000-3665.2011.05.003.

[20] Z.P. Song, Y.B. Qi, and N. Li, "Numerical analysis of the influence of concealed cave on the stability of circular tunnel", *Rock and Soil Mechanics*, vol. 28, pp. 485–489, 2007, doi: 10.16285/j.rsm.2007.s1.029.

[21] W.B. Peng, *Flac 3D Practical Tutorial*. Beijing: Machinery Industry Press, 2007.

[22] Z.H. Liang, X.N. Yang, and X.H. Jiang, "Study on construction mechanical characteristics of transition structure of separated repair in high speed railway tunnel", *Journal of East China Jiaotong University*, vol. 34, no. 6, pp. 26–31, 2017, doi: 10.16749/j.cnki.jecjtu.2017.06.002.

[23] Y.Q. Tang, "Study on spatial effect of unloading deformation of surrounding rock in large section soft rock tunnel excavation", M.A. thesis, East China Jiaotong University, Nanchang, 2019.

[24] JTG3370.1-2018 Design Specification for Highway Tunnels, vol. 1. Civil Engineering. China, People's Communications Publishing House Co., Ltd., 2019.

[25] C.C. Yao, H.L. Yu, and Y. Zhang, "A method for calculating the safety factor of lining strength based on Flac3D software", *Sichuan Architecture*, vol. 27, no. 2, pp. 115–116, 2007.

Received: 2024-05-08, Revised: 2024-11-12